ELSEVIER

Surface Science 393 (1997) 194–204

surface science

On kinetic phase transition of the dimer–monomer reaction model

Zhonghuai Hou, Lingfa Yang, Houwen Xin *

Department of Chemical Physics, University of Science and Technology of China, Hefei, Anhui 230026, China

Received 29 October 1996; accepted for publication 1 July 1997

Abstract

A detailed mean field theory (MFT) based on pair approximation (PA) is constructed to illustrate the kinetic phase transition behavior of the dimer–monomer surface reaction model $A+\frac{1}{2}B_2 \rightarrow AB$ and its variants which take into account diffusion and desorption of both adsorbed species, Eley–Rideal reaction step, finite reaction probability and "endon mechanism" for B_2 adsorption. We find that the PA-MFT can reproduce well the phase diagrams and yield quite good predictions of the effects of diffusion, desorption etc., which indicates that PA-MFT may be suitable for the description of the steady state behavior of this model. © 1997 Elsevier Science B.V.

Keywords: Kinetic phase transition; Mean field theory; Pair approximation

1. Introduction

The subject of reaction kinetics and phase transitions in surface catalysis is of great current interest and considerable effort has been devoted to the dimer–monomer (DM) reaction model $A+\frac{1}{2}B_2 \rightarrow AB$, which was originally known as the ZGB model based on the work of Ziff, Gulari and Barshad [1], where A and B_2 correspond to carbon monoxide (CO) and oxygen (O_2) respectively. In their Monte Carlo simulation (MCS), the monomers (A) adsorb at single empty sites on a square lattice at rate y_A (y_A is the mole fraction of the monomers in the gas phase), the dimers adsorb at adjacent pairs of empty sites at rate $y_B = 1 - y_A$, and different species adsorbed on adjacent sites react instantaneously with probability 1. Ziff et al. found two kinetic phase transitions with regard to y_A. For low values of y_A the surface is completely covered with B ($y_A \leq y_1 = 0.3905$) and for higher values with A ($y_A \geq y_2 = 0.525$). A reactive phase exists only in the "reactive window" $y_1 < y_A < y_2$ in which AB molecules are formed continuously. The phase transition at y_1 is of second order (continuous) and y_2 of first order (discontinuous). The decisive cooperative feature that leads to the phase transition behavior is the requirement that B_2 can be adsorbed only when there is a pair of neighboring empty sites [2].

These nonequilibrium phase transition behaviors can be understood, at least qualitatively by mean field theory (MFT) [2–8]. Two typical types of approximations are used in MFT: one is the site approximation (SA) [2–4] which neglects correlation and assumes random distribution of sites. For SA, the equations of motion are written for x_i (i=A, B or S, here S denotes the empty surface site), the concentration of adsorbed i sites, and the probability to find a pair of adjacent empty sites

* Corresponding author. Fax: (+86) 551 3603574; e-mail:hxin@ustc.edu.cn

PII S0039-6028(97)00586-4

is x_S^2. The other is the pair approximation (PA) or Bethe–Periles approximation [2,4–7], which considers the nearest-neighbor correlation and assumes random distribution of pairs i–j (i, j=A, B or S). Now, a set of coupled differential equations are derived for the pair concentrations x_{ij} and the probability to find a pair of empty sites is just x_{SS}. Both SA-MFT and PA-MFT can qualitatively predict the phase transition behavior, but PA-MFT yields more correct quantitative predictions of the values of y_1 and y_2, say, $y_1=0.2487$ and $y_2=0.5241$ for PA-MFT [4] and $y_1=0$ and $y_2=0.4787$ for SA-MFT [4] compared with the MCS values $y_1=0.3905$ and $y_2=0.525$. One sees that PA-MFT works quite well at y_2 but not y_1. That is comprehensible because the B-clusters near the second-order transition point are infinite, while both A-clusters and B-clusters are comparatively quite small year y_2 such that the PA is suitable for the description of the behavior near y_2 but not near y_1. The critical behaviors near y_1 and y_2 also show different features. The second-order transition belongs to the universality class of Reggon field theory (RFT) with critical behavior $\beta_B\theta_A \sim (y_A-y_1)^{\beta_A}$ and $(1-\theta_B)\sim(y_A-y_1)^{\beta_A}$, where θ_A and θ_B denote the average coverage of A(a) and B(a) in the steady state; here A(a) and B(a) denote the adsorbed monomer and dimer respectively, and $\beta_A=\beta_B=0.58$ [9–12]. "Oxidation epidemic" analysis and studies of the transient behavior near y_2, however, yield a different scaling relation: $\tau_A \propto |y_A-y_2|^{-\gamma}$ with $\gamma=3.54$ [13], where τ_A is the average relaxation time to A-poisoning.

Subsequent studies of the ZGB model have considered the influences of diffusion of A(a) and B(a) [3,5,9,14–16], the desorption of A(a) or B(a) [2,7,14,15,17–20], different initial conditions [3,5] and finite reaction probability (P_r) [7,14,15,21,22]. Other variants of the ZGB model have studied the effects of the "Eley–Rideal (ER)" [23,24] reaction step and "endon mechanism" for B_2 adsorption [10]. Since the original ZGB model corresponds to the carbon monoxide (CO) oxidation reaction $CO+\frac{1}{2}O_2\rightarrow CO_2$, the diffusion and desorption of O_2 are always neglected in MCS. However, as the DM model is so general that it does not represent any specific reaction system, the study of B-diffusion, B-desorption and other effects, using the MCS method or MFT analysis, should be helpful to the study of nonequilibrium kinetic phase transition behaviors.

Many authors have studied the influence of A-diffusion using the MCS method [3,14,15]. They found that A-diffusion markedly alters the values of y_2 but has no effect on the second-order transition point y_1. A higher diffusion rate shifts y_2 to higher value, and for infinite diffusion rate y_2 asymptotically approaches the stoichiometric value $\frac{2}{3}$. An extended version for the ZGB model has also considered B-diffusion [5,9]. One finds that B-diffusion both reduces y_1 sharply and shifts y_2 to the right, and for infinite diffusion rates of both A(a) and B(a), y_2 also seems asymptotically to be $\frac{2}{3}$ (Evans argued that the value of y_2 should be 0.595 at the high diffusion limit [16]). An extended version of PA-MFT [5] has been constructed to illustrate the influence of both A(a) and B(a) diffusion and the results are in good agreement with the MCS.

The behavior of the model changes accordingly if A(a) desorbs. When Dp_A (the desorption coefficient of species A) is below a critical value $Dp_A^* \simeq =0.04$, according to simulation, steady state hysteresis occurs [7,17,19] and there exists a first order transition from a low-θ_A state to a high-θ_A state at y_2' which is slightly larger than $y_2=0.525$. When $Dp_A > Dp_A^*$, the first-order phase transition disappears and the final coverage of A(a) is $1/(1+Dp_A)$ for $y_A=1$ [14,15]. Some authors have also studied the effects of A-desorption by theoretical approaches: in Ref. [17], the authors determined the value of Dp_A^* to be 0.214 by SA-MFT; in Ref. [19], Evans obtained a critical value $Dp_A \simeq 0.142$ for high surface mobility; and in Ref. [20], Dickman argued that, when A-desorption is considered, the A-poisoning belongs to Ising universality class. Although the desorption of B(a) is always neglected in computer simulation, it can also be studied by SA-MFT [2], but the effect of B-desorption were not discussed in detail in previous studies.

The initial condition of the lattice strongly affects the determination of the value of y_2. According to Ziff et al., the first-order transition

point $y_2=0.525$ is determined from the simulation on a square lattice initially half empty and half saturated by A(a). If evolving from an initially empty lattice, the value of y_2 is found to be 0.5277 [3,25]. Mai et al. [3] have carefully studied the influences of the initial condition by MCS. They found that a higher initial coverage of A(a), θ_A^0, reduces y_2 to a lower value, but a non-zero θ_B^0 does not alter y_2. On the other hand, the effects of θ_B^0 on y_2 can be eliminated by an equal θ_B^0 if A(a) can diffuse at a high rate. In Ref. [5], the authors have determined the values of y_2 by PA-MFT for two different initial conditions: $\theta_{AA}^0=\theta_{BB}^0=0$ and $\theta_{AA}^0=\theta_{SS}^0=0.5$ (with all other bond concentrations zero for both cases). The results are in reasonable agreements with the MCS results, but a detailed discussion of initial-condition effects were not performed.

In the above discussion, the reaction model is "adsorption controlled", i.e. after each adsorption step of A or B_2, the reaction takes place instantaneously if A(a) has nearest-neighboring B(a) or vice versa. The contrary case, when the model is "reaction controlled", has also been studied [21,22,7,14,15]. In this case, the model contains two elementary steps, namely, adsorption and reaction with probability $1-P_r$ and P_r (when $P_r=1$, this corresponds to the "adsorption-controlled" case). When P_r is reduced from 1, the reaction window is shifted left and becomes narrowed. In Ref. [21], the authors reported a tricritical point for P_r, $P_c\simeq 0.14$, below which there is no reactive state; however, according to Ref. [22], neither MCS nor MFT support this result, and the author pointed out that the existence of a tricritical point in Ref. [21] might be due to the fluctuation in the MCS.

For the original ZGB model, the reaction takes place according to the Langmuir–Hinshelwood (LH) mechanism, i.e. only different *adsorbed* species can react if they are nearest neighbors. In another variant of the ZGB model, the ER reaction mechanism has also been considered:

$$A(g)+B(a)\rightarrow AB(g)+S$$

namely, the monomer in the gas phase, A(g), can react with the adsorbed dimer, B(a), upon collision. MCS show that the second-order phase transition disappears and the first-order transition point now lies at $y_2^*=0.4975$ [24]. In the reaction interval $0\le y_A\le y_2^*$, the reaction rate is proportional to y_A.

As mentioned in the first paragraph, the decisive feature which leads to the phase transition behavior is the requirement of a pair of adjacent empty sites for B_2 adsorption. Evans et al. [10] have remarked on the sensitivity of the steady state behavior to the choice of B_2 adsorption mechanism. After randomly picking an empty site, the other site can be randomly chosen either from all the four neighbors (B_2 is adsorbed if empty), or from amongst only empty neighbors (if one or more exist). For the latter "endon mechanism", the authors find a narrow reaction window with $y_1=0.635$ and $y_2=0.655$.

We have given above a brief summary of recent studies on the ZGB model and its variants. The aim of this work is to construct a detailed MFT, especially using PA, to help in understanding the steady state behavior of this reaction model. In Section 2, the MFT which takes into account diffusion, desorption, finite probability, ER step and "endon mechanism" is constructed together with the main results and discussions. Our conclusions are given in Section 3.

2. Mean field theory

The SA-MFT and PA-MFT for the original ZGB model were constructed by Dickman [4]. For extended versions of the ZGB model, one should also describe the effects of diffusion, desorption, finite probability, the ER step and the "endon mechanism" in the equations of motion. As mentioned in Section 2, SA-MFT does not yield good predictions of the values of y_1 and y_2, and PA-MFT, which considers nearest-neighbor correlation, is suitable to describe the phase transition behavior of this model, especially at the first-order transition point. In this section, we just construct PA-MFT for extended ZGB models and the equations of motion based on SA-MFT are given in Appendix A.

The basic idea of PA-MFT is to derive the equations of motion for concentrations x_{ij} ($i, j=$

A, B or S) of allowed adjacent pairs or bonds. If the model is "adsorption controlled", namely, $P_r = 1$, then AB is removed from the surface immediately upon formation, so there are five pairs: S–S, A–S, B–S, A–A and B–B. Hence the time development of the system can be described by a set of four coupled differential equations for x_{ij} because the five concentrations add up to one. When the model is also "reaction controlled", A–B pairs must also be considered. In the present work, we first set the reaction probability to be 1 and study the steady-state behavior of extended ZGB models by PA-MFT, and we then investigate the finite-P_r case.

2.1. Adsorption controlled $P_r = 1$

To analyze the kinetics of the original ZGB model, one distinguishes between the following five processes:

(a) $B_2\downarrow$,
(b) $B_2\downarrow$, $AB\uparrow$,
(c) $B_2\downarrow$, $2AB\uparrow$,
(d) $A\downarrow$,
(e) $A\downarrow$, $AB\uparrow$,

where $\downarrow$ refers to adsorption and $\uparrow$ means that AB is generated and removed from the surface. To derive the equations of motion, one calculates the rates and changes in bond numbers for each process, and one has to distinguish both between different subprocesses leading to different bond-number changes and between the different configurations which might lead to a given process. Table 1 lists the subprocesses in schematic form and their rates. More details of the calculation can be found in Ref. [4]. One should note that there were some misprints for ΔN_{ij} listed in Table 1 therein. So we re-list the bond-number changes ΔN_{ij} in Table 2 for the convenience of further calculation.

Several other processes must be considered if the adsorbed species diffuse [5]:

(f) A(a)→,
(g) A(a)→, AB↑,
(h) B(a)→,
(i) B(a)→, AB↑.

The subprocesses and their rates are also listed in Table 1 and the bond-number changes can be found in Ref. [5]. We should remark here that the effective diffusion coefficient is sensitive to the diffusion mechanism. In MCS, after each adsorption trial, the diffusion step is repeated N_d times (N_d corresponds to $P_D/(1-P_D)$ in Ref. [5]). After randomly picking one adsorbed dimer or monomer, the adjacent empty site for diffusion can be selected either from all the four nearest neighbors [3,5,9,15] or from only empty nearest neighbors [14] (if one or more exist). We may call the first case homogeneous diffusion (HD) and the second one biased diffusion (BD). For HD case, the diffusion rate reads $N_{d_i} x_i x_{iS}/2x_i$ (i=A or B), where $x_{iS}/2x_i$ is the probability of finding an empty site among the nearest neighbors of i according to the PA. For the BD case, the diffusion rate is

Table 1
Rates and schematic forms for adsorption and diffusion processes. In processes (b2), (g1) and (i1), the three adsorbed species are on the same line, but in (b1, (g2) and (i2) they are not. In processes (c1), the two monomers A are nearest neighbours but in (c2) they are not (see Refs. [4,5]). In addition, the * in (b1), (g2) and (i2) must be S (empty site) which should be taken into account in the calculation of ΔN_{ij}[a]

Process	Diagram	Rates $R^{(k)}$
(a)	$SS \rightarrow BB$	$s_B(1-\mu)^6$
(b1)	$\begin{matrix} SS \\ *A \end{matrix} \rightarrow \begin{matrix} BB \\ *A \end{matrix} \overset{AB}{\rightarrow} \begin{matrix} BS \\ *S \end{matrix}$	$4s_B\mu(1-\mu)^3(1-\mu+\mu^2/3)$
(b2)	$SSA \rightarrow BBA \overset{AB}{\rightarrow} BSS$	$\frac{1}{2}R^{(b1)}$
(c1)	$\begin{matrix} SS \\ AA \end{matrix} \rightarrow \begin{matrix} BB \\ AA \end{matrix} \overset{2AB}{\rightarrow} \begin{matrix} SS \\ SS \end{matrix}$	$s_B\mu^2(2-4\mu+\frac{10}{3}\mu^2-\frac{4}{3}\mu^3+\frac{1}{6}\mu^4)$
(c2)	$\begin{matrix} ASS \\ A \end{matrix} \rightarrow \begin{matrix} ABB \\ A \end{matrix} \overset{2AB}{\rightarrow} \begin{matrix} SSS \\ S \end{matrix}$	$\frac{7}{2}R^{(c1)}$
(d)	$S \rightarrow A$	$y_A x_S(1-\nu)^4$
(e)	$SB \rightarrow AB \overset{AB}{\rightarrow} SS$	$y_A x_S[1-(1-\nu)^4]$
(f)	$AS \rightarrow SA$	$Rd_A(1-\nu)^3$
(g1)	$ASB \rightarrow SAB \overset{AB}{\rightarrow} SSS$	$Rd_A\nu(1-\nu+\nu^2/3)$
(g2)	$\begin{matrix} AS \\ *B \end{matrix} \rightarrow \begin{matrix} SA \\ *B \end{matrix} \overset{AB}{\rightarrow} \begin{matrix} SS \\ *S \end{matrix}$	$2R^{(g1)}$
(h)	$BS \rightarrow SB$	$Rd_B(1-\mu)^3$
(i1)	$BSA \rightarrow SBA \overset{AB}{\rightarrow} SSS$	$Rd_B\mu(1-\mu+\mu^2/3)$
(i2)	$\begin{matrix} BS \\ *A \end{matrix} \rightarrow \begin{matrix} SB \\ *A \end{matrix} \overset{AB}{\rightarrow} \begin{matrix} SS \\ *S \end{matrix}$	$2R^{(i1)}$

[a] $S_B = y_B x_{SS}$, if not "endon", $s_B = y_B x_S[1-(1-x_{SS}/x_S)^4]$, if "endon". $Rd_i = Nd_i \frac{1}{2} x_{iS}$ for HD case, $Rd_i = ND_i x_i[(1-(x_{ii}/x_i)^4]$, *for BD case* ($i = A$ *or* B). $\mu = x_{AS}/2x_S$, $\nu = x_{BS}/2x_S$.

Table 2
Bond-number changes for adsorption processes (see also Ref. [3]). The ΔN_{ij} for diffusion processes are not listed here (see Ref. [5])[a]

Process	ΔN_{SS}	ΔN_{SA}	ΔN_{SB}	ΔN_{BB}
(a)	$-1-12\alpha x_{SS}$	0	$6\alpha(2x_{SS}-x_{SB})$	$1+6\alpha x_{SB}$
(b1)	$\frac{x_{SA}}{x_A}-4\alpha x_{SS}$	$-2-\frac{x_{SA}}{x_A}+\frac{2x_{AA}}{x_A}$	$2-2\alpha x_{SB}+4\alpha x_{SS}$	$2\alpha x_{SB}$
(b2)	$-6\alpha x_{SS}+\frac{3x_{SA}}{2x_A}$	$-1-\frac{3x_{SA}}{2x_A}+\frac{3x_{AA}}{x_A}$	$1+6\alpha x_{SS}-3\alpha x_{SB}$	$3\alpha x_{SB}$
(c1)	$3+\frac{2x_{SA}}{x_A}$	$-2-\frac{2x_{SA}}{x_A}+\frac{4x_{AA}}{x_A}$	0	0
(c2)	$2+\frac{3x_{SA}}{x_A}$	$-2-\frac{3x_{SA}}{x_A}+\frac{6x_{AA}}{x_A}$	0	0
(d)	$-8\beta x_{SS}$	$-4\beta x_{SA}+8\beta x_{SS}$	0	0
(e)	$1+\frac{3x_{SB}}{2x_B}$	0	$-1+\frac{3x_{BB}}{x_B}-\frac{3x_{SB}}{2x_B}$	$-\frac{3x_{BB}}{x_B}$

[a] $\alpha=(2x_{SS}+x_{SB})^{-1}$. $x_j=\frac{1}{2}(2x_{jj}+\sum_{i\neq j}x_{ij})$ $(i,j=\text{A, B or S})$. $\beta=(2x_{SS}+x_{SA})^{-1}$.

$N_{d_i}x_i[1-(x_{ii}/x_i)^4]$, where $1-(x_{ii}/x_i)^4$ denotes the probability that there exists at least one empty site among the nearest neighbors of i, given that the neighbor cannot be the other species j (if $i=$A, then $j=$B and vice versa). So the effective diffusion coefficient for the BD case is greater than that for the HD case and they would lead to different quantitative predictions of the values of y_1 and y_2 but no difference in the qualitative steady state behavior.

For complete description of the model, we further consider the following processes:
(j) A↑, A desorption,
(k) B_2↑, B desorption,
(l) A(g)+B(a),AB↑, ER step.
The rates and bond-number changes according to the PA for these processes are shown in Table 3.

The equations of motion describing the development of the system are given by

$$\frac{dx_{ij}}{dt}=\sum_k R^{(k)}\,\Delta N_{ij}^{(k)}, \tag{1}$$

where $R^{(k)}$ is the rate of process k and $\Delta N_{ij}^{(k)}$ is the corresponding bond-number change of ij-pairs ($i,j=$A, B or S). The reaction rate of AB reads

$$R^{(AB)}=R^{(b)}+2R^{(c)}+R^{(e)}+R^{(g)}+R^{(i)}+R^{(l)}. \tag{2}$$

From numerical integration of these equations, we can readily study the steady state behavior of the DM model under the influences of diffusion, desorption, initial condition, ER mechanism and endon mechanism.

Table 3
Rates and bond-number changes for desorption processes and ER step. Dp_A and Dp_B are the desorption coefficients for A and B respectively

Process	Rate	ΔN_{SS}	ΔN_{AS}	ΔN_{BS}	ΔN_{BB}
(j)	$x_A Dp_A$	$\frac{2x_{AS}}{x_A}$	$\frac{4x_{AS}}{x_A}-\frac{2x_{AS}}{x_A}$	0	0
(k)	$x_{BB}Dp_B$	$1+\frac{3x_{BS}}{x_B}$	0	$\frac{6x_{BB}}{x_B}-\frac{3x_{BS}}{x_B}$	$-1-\frac{6x_{BB}}{x_B}$
(l)	$x_B y_A$	$\frac{2x_{BS}}{x_B}$	0	$\frac{4x_{BB}}{x_B}-\frac{2x_{BS}}{x_B}$	$-\frac{4x_{BB}}{x_B}$

2.1.1. Influences of diffusion

In Refs. [5,9], the times of diffusion attempts for each adsorption trial are the same for A and B ($N_{d_A}=N_{d_B}$). In the present work, we set $N_{d_A}\neq N_{d_B}$ and investigate their effects separately. The MFT results are listed in Table 4, where MCS results [3,5] are also listed. We adopt the HD mechanism for the calculation and the initial condition is $x_{SS}=1$ with all other bond concentrations zero. One sees that A-diffusion only shifts y_2 to the right and B-diffusion both reduces y_1 sharply and shifts y_2 to a larger value. This is in accordance with Refs. [5,9]. In addition, we find that equal diffusion rates of A and B lead to approximately the same drifts in the value of y_2. When diffusion is very fast, PA-MFT predicts $y_2\to\frac{2}{3}$, which seems to be in agreement with the simulation results of Refs. [3,13,14] but not with the theoretical analysis of Evans [16].

One expects that PA-MFT becomes more accurate when diffusion becomes faster because there is more randomization on the surface and the correlation is reduced. In Table 4, Δy_2 denotes the difference of y_2 value between PA-MFT and MCS which tend to be smaller when diffusion becomes faster.

2.1.2. Influence of initial condition

The values of y_2 depend strongly on the initial state of the lattice. For example, when the initial lattice is empty, y_2 is found to be 0.5277 compared with $y_2=0.525$ when the lattice is initially half empty and half saturated by A(a). Choosing different initial conditions for Eq. (1), we have studied these effects by PA-MFT. The values of the transition points obtained from MFT and MCS are both listed in Table 5 (the MCS values are mainly drawn from Ref. [3]). We find that PA-MFT correctly reproduces the qualitative features obtained by MCS that larger θ_A^0 leads to smaller y_2 and a non-zero θ_B^0 does not change y_2 and the effects of θ_A^0 can be eliminated by an equal θ_B^0 if A-diffusion is fast. On the other hand, the initial condition of the lattice has no influence on the value of y_1 and we have not listed the values of y_1 in Table 5.

Choosing initial condition $x_{ss}=1$ with all other bond concentrations zero, PA-MFT predicts a first-order transition at $y_A=0.561$ which is larger than the MCS value $y_2=0.5277$. In fact, 0.561 denotes the "spinodal" [5,6] point y_s of this

Table 5
The influence of initial state. The MCS results are taken from Ref. [3]

$(\theta_A^0,\theta_B^0$	y_2 (MCS) $(Nd_A=40)$	y_2 (PA-MFT) $(Nd_A=40)$	y_2 (PA-MFT) $(Nd_A=0)$
(0,0)	0.650 ± 0.001	0.6382	0.5610
$(\frac{1}{5},0)$	0.605 ± 0.001	0.6106	0.5556
$(\frac{1}{2},0)$	0.520 ± 0.002	0.5084	0.5241
$(\frac{2}{3},0)$	0.428 ± 0.002	0.4158	0.4965
$(\frac{3}{4},0)$	0.382 ± 0.004	0.3532	0.4787
$(\frac{1}{4},\frac{1}{4})$	0.648 ± 0.002	0.6375	0.5595
$(\frac{1}{5},\frac{2}{5})$	0.652 ± 0.002	0.6382	0.5610
$(\frac{2}{5},\frac{1}{5})$	0.605 ± 0.001	0.6061	0.5476
$(0,\frac{1}{5})$	0.649 ± 0.002	0.6382	0.5610

Table 4
The influences of A or B diffusion on the positions of the transition points. The initial state of the system is chosen to be the empty lattice. The MCS results are drawn from Refs. [3,15]. One expects, from the two rows labelled *, that PA-MFT predicts y_2 goes asymptotically to 2/3 when diffusion rates become infinite

(Nd_A,Nd_B)	y_1 (MCS)	y_2 (MCS)	y_1 (PA-MFT)	y_2 (A-MFT)	Δy_2
(0,0)	0.390	0.5277	0.2487	0.5610	0.0333
(10,0)	0.390	0.632	0.2487	0.6177	0.0143
(20,0)	0.390	0.640	0.2487	0.6288	0.0112
(40,0)	0.390	0.650	0.2487	0.6382	0.0118
*(4000,0)		$\to 2/3$		0.6633	≈ 0.003
(0,10)	–	–	<0.001	0.6178	
(0,40)	–	–	≈ 0	0.63	
*(0,4000)	–	–	≈ 0	0.6634	

system, and in the interval $y_2 < y_A < y_s$ there exists a "metastable" region in which MFT predicts a metastable reactive state rather than the actual A-poisoning state. Mai et al. argued [26–28] that this discrepancy results from the finite-size effect in MCS. In Refs. [1,4,18], the workers adopted the following kinetic criterion to determine the first-order transition point y_2 by considering the evolution from an initial state in which half of the lattice is empty and half saturated by A(a): for $y_A < y_2$, the initial condition evolves to a reactive steady state; while for $y_A > y_2$ to A-poisoning. Then $y_2 = 0.525$ is obtained by simulation. Choosing $x_{SS} = x_{AA} = 0.5$ as the initial condition of Eq. (1), one finds that PA-MFT predicts $y_2 = 0.5241$ which shows quite good agreement with the simulation.

2.1.3. *Effects of desorption*

As mentioned in Section 1, if the desorption coefficient of A(a), Dp_A is below a critical value Dp_A^*, there still exists a first-order transition from a low-θ_A state to a high-θ_A state; while above Dp_A^*, the phase transition disappears. In the present work, we find $Dp_A^* \simeq 0.155$ according to PA-MFT. This value is substantially higher than 0.04 [17,19] obtained by simulation, but it is somewhat better than 0.214 obtained from SA-MFT [17] and is also reasonable agreement with 0.142 obtained by Evans. Fig. 1(a) and (b) show the phase diagrams obtained by PA-MFT when Dp_A is slightly below and above Dp_A^*. When $Dp_A = 0.15$, the first-order transition occurs at $y_A = 0.5868$; and when $Dp_A = 0.16$, the variation of θ_A^s or θ_A^s with y_A is continuous and there is no phase transition near $y_s = 0.561$.

We have also studied the influences of B-desorption. A non-zero value of Dp_B removes the second-order transition but has no effect on the first-order transition. One does not find a critical value for Dp_B because no steady-state hysteresis exists near y_1. On the other hand, with increasing y_A from zero θ_B^s runs across a maximum. When y_A is zero, B-adsorption and B-desorption would be in equilibrium after the system reaches the steady state. However, θ_B^s is not $1/(1+Dp_B)$ because B-adsorption needs a pair of adjacent empty sites which causes a "jammed" effect. So

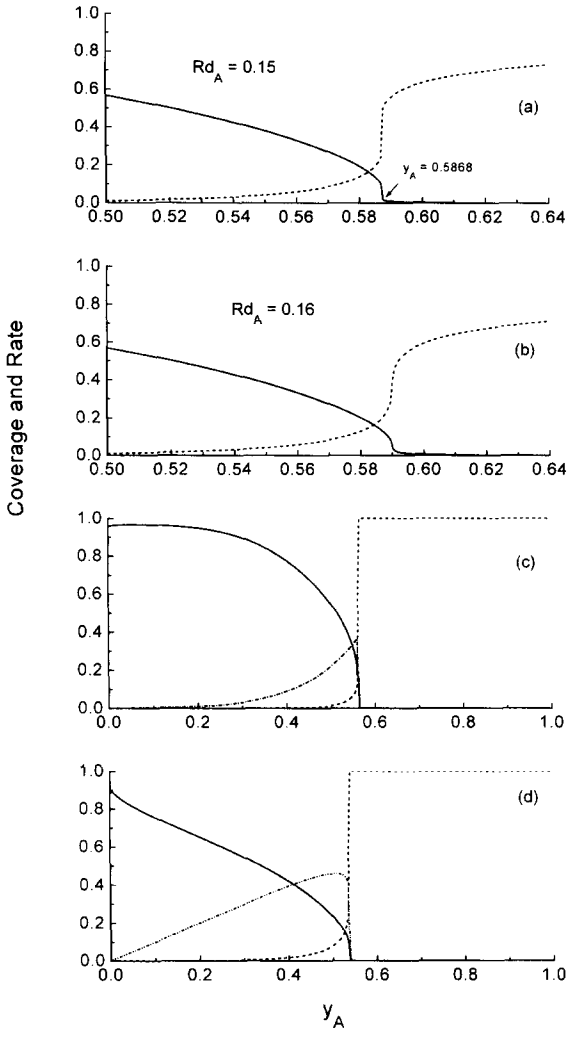

Fig. 1. Some phase diagrams obtained from PA-MFT: solid line: θ_B^s; dashed line: θ_A^s; dashed-dotted line: R_{AB}. (a) $Rd_A = 0.15$ which is slightly below $Rd_A^* = 0.155$. A first order transition occurs at $y_2 = 0.5868$. (b) $Rd_A = 0.16$. The phase transition disappears. (c) $Rd_B = 0.002$. One observes a maximum of θ_B^s at $y_A \simeq 0.06$. (d) The ER reaction step is considered. y_1 disappears and y_2 is 0.5375.

with y_A increasing from zero but not high, reaction occurs and the probability of B-adsorption is raised which may lead to the increase of θ_B^s. Of course, a further increased y_A will reduce θ_B^s and thus one observes a maximum of θ_B^s at a certain y_A. A typical phase diagram with $Dp_B = 0.002$ is shown in Fig. 1(c) where the maximum of θ_B^s lies at $y_A \simeq 0.06$.

2.1.4. Influences of ER step and "endon mechanism"

Taking into account the ER reaction step, PA-MFT predicts $y_2^* = 0.5375$ and the second-order phase transition disappears. This value is greater than 0.4975 obtained by Meakin [24]. However, $y_2 - y_2^*$, i.e the drift in the position of the first-order transition point from the original ZGB model to ER case, is $0.5610 - 0.5375 = 0.0235$, which is in good agreement with $0.525 - 0.4975 = 0.0275$ obtained by MCS. The reaction rate rises monotonically with y_A and the linear relationship between them can apparently be seen in Fig. 1(d).

If B_2 is adsorbed according to the "endon mechanism", the sticking probability should be $y_B x_S[1-(1-x_{SS}/x_S)^4]$ instead of $y_B x_{SS}$. PA-MFT predicts that $y_1 = 0.5095$ and $y_2 = 0.6628$ compared with $y_1 = 0.635$ and $y_2 = 0.655$ obtained by MCS. One finds again that PA-MFT works well at the first-order point but not at the second-order point.

2.2. Reaction controlled $P_r < 1$

The effects of finite reaction probability, say the model is also "reaction controlled", have also been discussed or studied in Refs. [21,22,7,14,15]. According to Refs. [21,22], the simulation contains two elementary steps: adsorption and reaction with probability $1-P_r$ and P_r respectively (so the "reaction–adsorption ratio" is $P_r/(1-P_r)$. In the adsorption step, the dimer B_2 or monomer A adsorbs with probability y_B or $1-y_B$, but now the nearest neighbors need not be checked for reaction since the reaction step is now treated separately. In the reaction step, one randomly picks a pair of sites and if it is of type A(a)–B(a), the pair is removed from the surface with probability 1. Thus according to PA-MFT, one can just distinguish between the following three processes:

(a) $A\downarrow$, $S \rightarrow A$,
(b) $B_2\downarrow$, $SS \rightarrow BB$,
(c) $AB\uparrow$, $AB \rightarrow SS$,

the rates of which are $(1-P_r)y_A x_S$, $(1-P_r)y_B x_{SS}$ and $P_r x_{AB}$ respectively.

In Ref. [14], the authors also realized the reaction step separately where they considered the interaction model when the reaction probability is dependent on temperature and the interaction energy between the two adsorbed species. However, the "reaction–adsorption ratio" there is 1 (which corresponds to $P_r = 0.5$ in the above case), and even if one picks an A(a)–B(a) pair the two species react with another probability p_r less than one. Thus, according to PA-MFT, the rates for the three processes: A-adsorption, B-adsorption and AB-reaction are $y_A x_S$, $y_B x_{SS}$ and $p_r x_{AB}$ respectively (we have normalized these rates by a factor $1/P_r$).

It is rather interesting to realize the finite reaction probability in another way, i.e. to consider the model with "instantaneous reaction" after each successful adsorption step with a probability p_r less than one. For example, when the monomer A is adsorbed, its nearest neighbors are checked for B(a) species, and the reaction takes place with probabilty $p_r \leq 1$ if one or more exist. Now, the processes that occur on the surface are more complicated than those listed in Table 1 since one should distinguish between "reaction" and "no reaction" when a newly adsorbed A species has B(a) nearest neighbors or vice versa. For example, for process (b1), the initial configuration S S A first becomes B B A after a successful adsorption of B_2, and then either changes to B S S with probability p_r (reaction) or remains to be B B A with probability $1-p_r$ (no reaction).

We may call the above three models M1, M2 and M3. For M1 and M2, the rates and bond-number changes are listed in Table 6. For M3, the subprocesses and the rates are presented in Table 7, and the bond-number changes that are not listed in Table 2 are also given in Table 6. The equations of motion are similar to Eq. (1). Our results obtained from PA-MFT are summarized in Fig. 2, where (a), (b) and (c) correspond to M1, M2 and M3 respectively. Notice here that the initial state of the surface is empty, so the top lines denote the spinodal values. One concludes from Fig. 2 that the reaction window becomes left shifted and narrowed when the reaction probability decreases.

For "separate reaction" models M1 and M2, we do not find a critical value for the reaction probability P_r or p_r, which supports the results obtained by Kohler and Ben-Avraham [22]. However, for "instantaneous reaction" model M3, there is a tricritical point at $p_r = 0.627 \pm 0.003$. In fact, for

Table 6
Rates and bond-number changes for "reaction-controlled" models. Processes a′, b′, c′ correspond to M1 and M2 and the other processes correspond to M3. Notice that, for M3, bond-number changes for subprocesses (a), (b1a), (b2a), (c1a), (c2a), (d), (e1) are presented in Table 2

Process	ΔN_{SS}	ΔN_{AS}	ΔN_{BS}	ΔN_{AA}	Δ_{BB}
(a′)	$-\frac{4x_{SS}}{x_S}$	$\frac{4x_{SS}}{x_S}-\frac{2x_{AS}}{x_S}$	$-\frac{2x_{BS}}{x_S}$	$\frac{2x_{AS}}{x_S}$	0
(b′)	$-1-\frac{6x_{SS}}{x_S}$	$-\frac{3x_{AS}}{x_S}$	$\frac{6x_{SS}}{x_S}-\frac{3x_{BS}}{x_S}$	0	$1+\frac{3x_{BS}}{x_S}$
(c′)	$1+\frac{3x_{AS}}{2x_A}+\frac{3x_{BS}}{2x_B}$	$\frac{3x_{AA}}{x_A}+\frac{3x_{AB}}{2x_B}-\frac{3x_{AB}}{2x_A}$	$\frac{3x_{BB}}{x_B}+\frac{3x_{AB}}{2x_A}-\frac{3x_{BS}}{2x_B}$	$-\frac{3x_{AA}}{x_A}$	$-\frac{3x_{BB}}{x_B}$
(b1b)	$-1-6\alpha x_{SS}+\frac{2x_{SS}}{x_S}$	$-1-\frac{x_{AS}}{x_S}$	$\left(3\alpha+\frac{1}{x_s}\right)(2x_{SS}-x_{BS})$	0	$1+3\alpha x_{BS}+\frac{x_{BS}}{x_S}$
(b2b)	$-1-6\alpha x_{SS}+\frac{2x_{SS}}{x_S}$	$-1-\frac{x_{AS}}{x_S}$	$\left(3\alpha+\frac{1}{x_S}\right)(2x_{SS}-x_{BS})$	0	$1+3\alpha x_{BS}+\frac{x_{BS}}{x_S}$
(c1b)	$\frac{x_{AS}}{x_A}-\frac{2x_{SS}}{x_S}$	$-1-\frac{x_{AS}}{S}+\frac{2x_{AA}-x_{AS}}{x_A}$	$1+\frac{2x_{SS}-x_{BS}}{x_S}+\frac{x_{AB}}{x_A}$	$-1-\frac{2x_{AA}}{x_A}$	$\frac{x_{BS}}{x_S}$
(c1c)	$-1-\frac{4x_{SS}}{x_S}$	$-2-\frac{2x_{AS}}{S}$	$\frac{4x_{SS}-2x_{BS}}{x_S}$	0	$1+\frac{2x_{BS}}{x_S}$
(c2b)	$\frac{3x_{AS}}{2x_A}-\frac{2x_{SS}}{x_S}$	$-2-\frac{x_{AS}}{S}+\frac{6x_{AA}-3x_{AS}}{2x_A}$	$1+\frac{2x_{SS}-x_{BS}}{x_S}+\frac{3x_{AB}}{2x_A}$	$-\frac{3x_{AA}}{x_A}$	$\frac{x_{BS}}{x_S}$
(c2c)	$-1-\frac{4x_{SS}}{x_S}$	$-2-\frac{2x_{AS}}{S}$	$\frac{4x_{SS}-2x_{BS}}{x_S}$	0	$1+\frac{2x_{BS}}{x_S}$
(e2)	$-\frac{3x_{SS}}{x_S}$	$-\frac{6x_{SS}-3x_{AS}}{2x_S}$	$-1-\frac{3x_{BS}}{2x_S}$	0	0

Table 7
Rates and schematic forms for adsorption and diffusion processes for the "reaction-controlled" model 3, where $R^{(k)}$s are drawn from Table 1

Process	Diagram	Rates $R^{(k)}$	Process	Diagram	Rates $R^{(k)}$
(a)	SS→BB	$s_B(1-\mu)^6$	(b1a)	$\overset{SS}{*A}\rightarrow\overset{BS}{*S}$	$\frac{1}{2}R^{(b1a)}$
(b1b)	$\overset{SS}{*A}\rightarrow\overset{BB}{*A}$	$\frac{1}{2}R^{(b1b)}$	(b2a)	SSA→BSS	$p_rR^{(b1)}$
(b2b)	SSA→BBA	$(1-p_r)R^{(b1)}$	(c1a)	$\overset{SS}{AA}\rightarrow\overset{SS}{SS}$	$p_r^2R^{(3a)}$
(c1b)	$\overset{SS}{AA}\rightarrow\overset{SB}{SA}$	$2p_r(1-p_r)R^{(3a)}$	(c1c)	$\overset{SS}{AA}\rightarrow\overset{BB}{AA}$	$(1-p_r)^2R^{(3a)}$
(c2a)	$\overset{ASS}{A}\rightarrow\overset{SSS}{S}$	$\frac{7}{2}R^{(c1a)}$	(c2b)	$\overset{ASS}{A}\rightarrow\overset{ABS}{S}$	$\frac{7}{2}R^{(c1b)}$
(c2c)	$\overset{ASS}{A}\rightarrow\overset{ABB}{A}$	$\frac{7}{2}R^{(c1c)}$	(d)	S→A	$R^{(d)}$
(e1)	SB→SS	$p_rR^{(e)}$	(e2)	SB→AB	$(1-p_r)R^{(e)}$

M1 and M2, although the reaction probability is rather small, the separate reaction step can remove the adjacent AB pairs and sustained reaction can occur between a certain interval of y_A; however, for M3, if the instantaneous reaction step does not succeed, the AB pair would stay on the surface until another possible reaction between either of them and another newly adsorbed species of a different type, and thus if the reaction probability is less than a critical value, the surface would be saturated by A(a), B(a) and "not-reacted" AB pairs such that no reaction window exists.

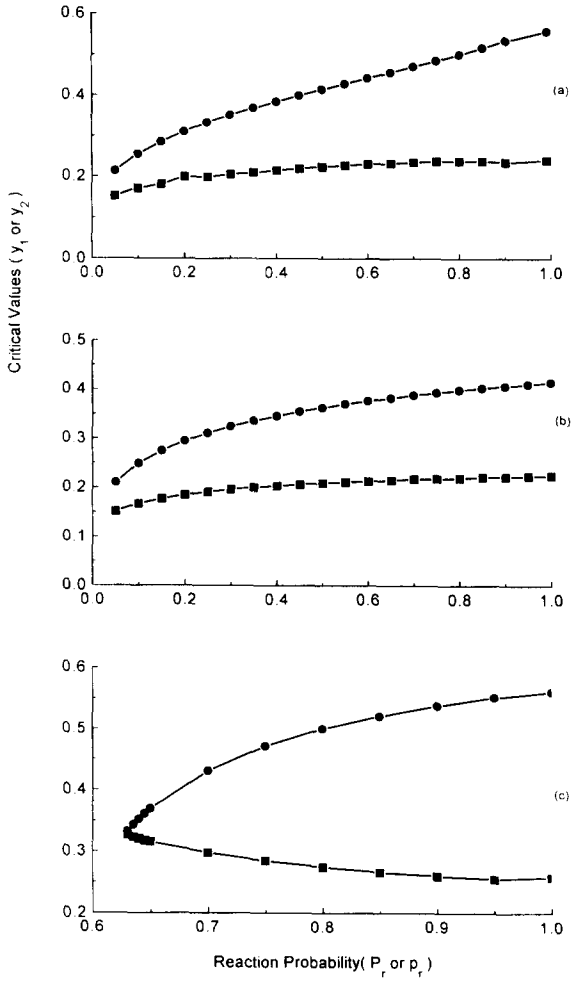

Fig. 2. Phase diagrams for "reaction controlled" case: ●, y_s; ■, y_1. (a) "Separate reaction" case M1; (b) "separate reaction" case M2; (c) "instantaneous reaction" case M3. For details, see the text.

One notes that there are also differences between M1 and M2. Near $P_r=1$, there is a good agreement between M1 and the original DM model, say y_1 and y_s asymptotically approach 0.2487 and 0.561. For M2, however, even when $p_r=1$, the values of y_1 and y_s are much lower than those of the original model, say $y_1=0.224$ and $y_2=0.415$. In fact, as discussed above, $p_r=1$ for M2 corresponds to $P_r=0.5$ for M1, when one can still find AB pairs on the surface, such that it does not agree with the original DM model. From this point of view, one may conclude that M2 is not suitable to describe the "reaction-controlled" model.

3. Conclusions

In the present work, we have constructed a detailed MFT to illustrate the kinetic phase transition behavior of the DM reaction model and its variants which take into account diffusion and desorption of both monomer and dimer, the ER reaction step, "endon mechanism" for B-adsorption and finite reaction probability. We find that PA-MFT can reproduce the MCS results qualitatively quite well, and even quantitatively well near the first-order transition point which indicates that PA-MFT is suitable to describe this kind of kinetic phase transition behavior. Additionally, one may predict new features of the model based on the equations of motion ahead of MCS.

Acknowledgements

This work is supported by the National Science Foundation of China.

Appendix A

The equations of motion derived from SA-MFT read:

$$\frac{dx_A}{dt} = -2s_B[1-(1-x_A)^3]+y_A x_S(1-x_B)^4 - Rd_A[1-(1-x_B)^3]-Rd_B[1-(1-x_A)^3] - Dp_A x_A \quad (A.1)$$

$$\frac{dx_B}{dt} = 2s_B(1-x_A)^3 - y_A x_S[1-(1-x_B)^4] - Rd_A[1-(1-x_B)^3]-Rd_B[1-(1-x_A)^3] - 2Dp_B x_B^2 - R_{er} y_A x_B \quad (A.2)$$

where s_B is the "sticking probability" of B_2 which reads $s_B = y_B x_S^2$ if one does not adopt the "endon

mechanism" for B_2 adsorption or else $s_B = y_B x_S[1-(1-x_S)^4]$. For the HD case, Rd_i reads $Nd_i x_i x_S/(x_i + x_S)$, where $x_S/(x_i + x_S)$ is the probability to find an empty site among the four nearest neighbors of site i given that the neighbor cannot be the other adsorbed species j (for $i=A$, $j=B$ and vice versa); and for BD case, Rd_i is $Rd_i x_i(1-x_i^4)$. If one considers the ER reaction step, then R_{er} reads 1 or else it is 0.

References

[1] R.M. Ziff, E. Gulari, Y. Barshad, Phys. Rev. Lett. 56 (1986) 2553.
[2] P. Fischer, V.M. Titulaer, Surf. Sci. 221 (1989) 409.
[3] J. Mai, W. Von Niessen, A. Blumen, J. Chem. Phys. 93 (5) (1990) 3685.
[4] R. Dickman, Phys. Rev. A 34 (5) (1986) 4246.
[5] I. Jensen, H.C. Fogedby, Phys. Rev. A 42 (4) (1990) 1969.
[6] J.W. Evans, M.S. Niesch, Surf. Sci. 245 (1991) 401.
[7] M. Dumont, P. Dufour, B. Sente, R. Dagonnier, J. Catal. 122 (1990) 95.
[8] P. Araya, W. Porod, R. Sant, E.E. Wolf, Surf. Sci. 208 (1989) L80.
[9] L.V. Lutsevich, V.I. Elokhin, A.V. Myshlyavtsev, A.G. Usov, G.S. Yablonskii, J. Catal. 132 (1991) 302.
[10] J.W. Evans, M.S. Miesch, Phys. Rev. Lett. 66 (1991) 833.
[11] R. Dickman, I. Jensen, H.C. Fogedby, Phys. Rev. A 41 (6) (1990) 3411.
[12] G. Gristein, Z.W. Lai, D.A. Browne, Phys. Rev. A 40 (1989) 4820.
[13] K. Yaldram, A. Sadiq, J. Phys. A Maths. Gen. 22 (1989) L925–L929.
[14] H.P. Kaukonen, R.M. Nieminen, J. Chem. Phys. 91 (1989) 4380.
[15] M. Ehsasi, M. Matoich, O. Frank, J.H. Block, J. Chem. Phys. 91 (8) (1989) 4949.
[16] J.W. Evans, J. Chem. Phys. 98 (3) (1993) 2463.
[17] B.J. Brosilow, R.M. Ziff, Phys. Rev. A 46 (1992) 4534.
[18] R.M. Ziff, B.J. Brosilow, Phys. Rev. A 46 (1992) 4630.
[19] J.W. Evans, J. Chem. Phys. 97 (1992) 572.
[20] T. Tome, R. Dickman, Phys. Rev. E 47 (1993) 948.
[21] D. Considine, H. Takkayasu, S. Redner, J. Phys. A 23 (1990) L1181.
[22] J. Kohler, D. Ben-Avraham, J. Phys. A 25 (1992) L141.
[23] S.S. Tambe, V.K. Jayaraman, B.D. Kulkarni, Chem. Phys. Lett. 225 (1994) 303.
[24] P. Meakin, J. Chem. Phys. 93 (1990) 2903.
[25] P. Meakin, D.J. Scalapino, J. Chem. Phys. 87 (1987) 731.
[26] J. Mai, V.N. Kuzovkov, W. Von Niessen, Physica A 203 (1994) 298–315.
[27] J. Mai, V.N. Kuzovkov, W. Von Niessen, J. Chem. Phys. 100 (1994) 6073.
[28] J. Mai, V.N. Kuzovkov, W. Von Niessen, J. Chem. Phys. 100 (1994) 8522.